

A Computational Approach for Simulating P-type Silicon Piezoresistor Using Four Point Bending Setup

T. H. Tan^{*1}, S.J.N Mitchell¹, D.W. McNeill¹, H. Wadsworth² and S. Strahan²

¹ Queen's University Belfast, Belfast, UK, ² Schrader Electronics Ltd, Antrim, UK

^{*}School of Electronics, Electrical Engineering and Computer Science, Queen's University Belfast, BT9 5AH, United Kingdom, ttan05@qub.ac.uk

Abstract: The piezoresistance effect is defined as change in resistance due to applied stress. Silicon has a relatively large piezoresistance effect which has been known since 1954. A four point bending setup is proposed and designed to analyze the piezoresistance effect in *p*-type silicon. This setup is used to apply uniform and uniaxial stress along the <110> crystal direction. The main aim of this work is to investigate the piezoresistive characteristic of *p*-type resistors as a function of doping concentrations using COMSOL Multiphysics. Simulation results are compared with experimental data.

Keywords: piezoresistance, four point bending setup, *p*-type silicon, COMSOL Multiphysics, FEM model.

1. Introduction

Silicon piezoresistive sensors are widely used in MEMS sensing applications since the discovery of this technology by Smith in 1954 [1]. The piezoresistance effect is defined as change in resistance when subjected to stress. Piezoresistive MEMS sensors are commercially available in various applications namely pressure sensor, accelerometer, cantilever force/displacement sensors, etc [2]. In order to optimize the sensitivity of a piezoresistive sensor, numerical simulations such as finite element methods (FEM) are employed to estimate the piezoresistive effect under various stress conditions. The orientation of the piezoresistive sensing structure and doping level have significant influence on the resulting piezoresistance effect.

2. Theory

The theory of piezoresistive effect is closely related to the conductivity of the semiconductor material. Hence, the expression in E , Electric field can be expressed in [1]

$$E = \rho \cdot J + \Delta\rho \cdot J \quad (1)$$

where J is the current, ρ is the resistivity and $\Delta\rho$ is the relative change in resistivity due to the applied stress. The relative change in resistivity is defined as [1]

$$\Delta\rho = \pi \cdot \sigma \quad (2)$$

where π is the piezoresistance tensor (units in Pa^{-1}) and σ is the stress. Effectively, the relative change in resistivity is proportional to the relative change in resistance. Hence, the resistance change for a piezoresistor can be derived as the function of the longitudinal and transverse stresses as below [3,4,5,6]

$$\frac{\Delta\rho}{\rho} = \frac{\Delta R}{R} = \pi_l \sigma_l + \pi_t \sigma_t \quad (3)$$

π_l and π_t are longitudinal and transverse piezoresistive coefficients; σ_l and σ_t are longitudinal and transverse stress respectively. Since four point bending produces uniaxial stress (dominant in longitudinal direction), the stress in transverse can be neglected in this equation to form [3,4,5,6]

$$\frac{\Delta R}{R} \cong \pi_l \sigma_l \quad (4)$$

The effective piezoresistive coefficient (π_l) can be determined by measuring the three piezoresistive coefficients in silicon ie. π_{11} , π_{12} , and π_{44} . By applying a uniaxial stress along the <110> direction in *p*-type silicon, the equation can be further simplified to [3,4,5,6]

$$\pi_l = \frac{1}{2}(\pi_{11} + \pi_{12} + \pi_{44}) \approx \frac{1}{2}\pi_{44} \quad (5)$$

Table 1 presents the typical room temperature values of the piezoresistive coefficient for lightly doped silicon. It is obvious that π_{44} is much larger than π_{11} and π_{12} , hence they could be neglected as deduced in Eq. (5).

Resistivity	π_{11}	π_{12}	π_{44}
7.8Ω-cm, <i>p</i> -type	6.6	-1.1	138.1

Table 1: Room-temperature piezoresistive coefficients for silicon at 10^{11} Pa^{-1} [1].

The dependence of piezoresistive coefficient $\pi(N,T)$ with impurity concentration N and temperature T can be written as [7]

$$\pi(N,T) = P(N,T) \cdot \pi(300K) \quad (6)$$

where $P(N,T)$ is the piezoresistance factor. In this work, a four point bending (4PB) apparatus is employed to produce uniaxial and uniform stress

on a silicon beam. The centre stress, σ_c , can be determined by [3,4,5,6]

$$\sigma_c = \frac{3Fa}{wt^2} \quad (7)$$

where F is the force, a is the distance between the supports, w is the width of the beam, and t is the thickness of the beam. Deflection at the loading point, z , can be determined by [3,4,5,6]

$$z = \frac{(12aL-16a^2)aF}{4Et^3w} \quad (8)$$

where L is the distance between the outer supports, E is the Young's modulus of material. Both stress and deflection equations hold, provided that the deformation of the beam is small. **Figure 1** illustrates the fabricated silicon beam where piezoresistors are located at the top centre surface. Force is subsequently applied onto the silicon beam using a four point bending fixture which is demonstrated in **Figure 2**. [6]



Figure 1: Overview of fabricated silicon beam array with piezoresistors at the surface of silicon beam. [4]

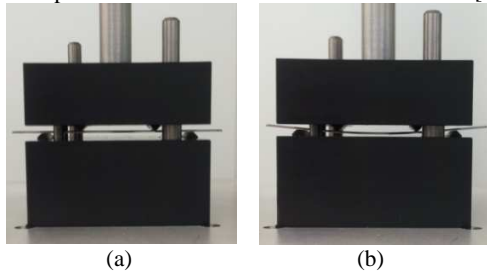


Figure 2: Fabricated four point bending fixture in action. (a)zero load (b)1500g load. [4]

3. COMSOL Multiphysics simulation

A four point bending setup is modeled using COMSOL Multiphysics 4.3. The 3D geometry comprises three main components including a top support block, bottom support block and silicon beam (as depicted in **Figure 3**). The support blocks are both made of plastic (Delrin 500). The dimension of the silicon bar is 40mm long, 6mm wide and 400 μ m thick. **Table 2** presents the properties of silicon used in this simulation. From **Figure 3**, it can also be seen that two inner blades and outer blades with separation of 14mm and 28mm apply the loading forces to the silicon beam.

A 2 mm square area is allocated at the centre top surface of the silicon beam for placement of the silicon piezoresistors (as demonstrated in **Figure 4**). A newly introduced user interface in COMSOL Multiphysics 4.3 has enabled users to perform simulation for piezoresistivity in semiconductor materials such as single crystal silicon. To investigate the piezoresistance effect, a two terminal resistor configuration with dimension of 500 \times 20 μ m is included to determine the resistance change when the silicon beam is subjected to external loading.

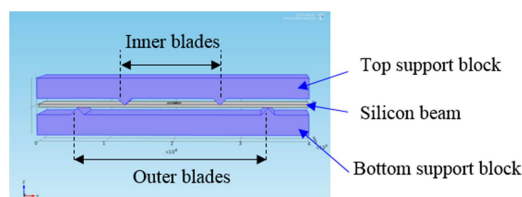


Figure 3: 3D geometry of four point bending setup.

Silicon Properties	Descriptions
Young's modulus	160GPa
Poisson's ratio	0.28

Table 2: fundamental properties of silicon used in simulation. [6,8]

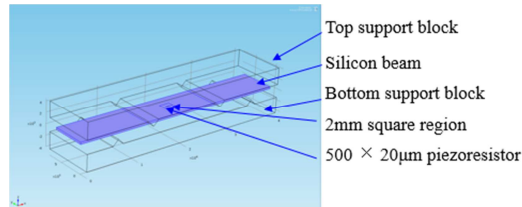


Figure 4: Location of 2 mm square and piezoresistor at the surface of silicon beam.

Figure 5 illustrates the design of the two terminal piezoresistor including the two contact pads with similar dimensions. Inclusion of a thin conductive layer is important when setting up a piezoresistive model to ensure that the current flows through the material with a constant conductivity. It was found that keeping the conductive pads the same size as the resistor gives the best results. It was also observed that the doping concentration and the dimension of contact pad can influence the piezoresistance effect for all resistors.

The thickness of the resistor is defined as 1 μ m. Four different doping concentration values are used for the piezoresistors namely; 1.0 $\times 10^{19}$ cm $^{-3}$, 7.6 $\times 10^{19}$ cm $^{-3}$, 1.2 $\times 10^{20}$ cm $^{-3}$ and

$1.3 \times 10^{20} \text{cm}^{-3}$. A thin conductive layer with doping concentration of $1.5 \times 10^{20} \text{cm}^{-3}$ is defined for the contact regions. A voltage of 3V is supplied from one edge while the opposite edge of the other contact pad is connected to ground. To ensure the resistor is orientated in $\langle 110 \rangle$ direction, global coordinate is modified to match the orientation.

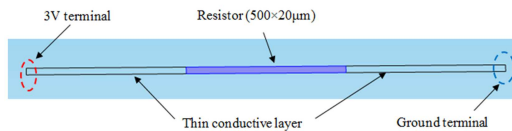


Figure 5: Two terminal configuration resistor
The meshing is designed to be finer around the piezoresistor area. **Figure 6** depicts the meshing density on the top surface of the silicon bar.

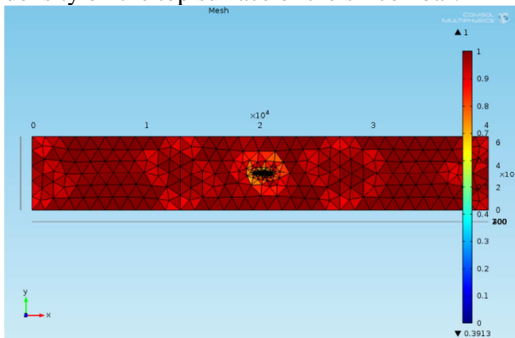


Figure 6: Meshing of silicon bar (top surface).

4. Results

During simulation, a downward force is applied to the silicon beam; the resultant displacement and stress are recorded. Stress distribution in the x direction is demonstrated in **Figure 7**. **Figure 8** illustrates the principle stresses across the length of a silicon bar subjected to a 3N downwards force. It can be observed that the centre stress at the surface of silicon beam between the two inner supports is uniform and uniaxial (dominated by stress in the x direction).

Potential distribution for 3V input across the resistor is illustrated in **Figure 9**. To determine the piezoresistive effect, resistance change data for each doping level are plotted and analysed. **Figure 10** depicts the change in resistance as a function of force up to 3N for the four doping concentration values. The result demonstrates that the resistance change is linearly proportional to applied stress for small force application. Results also show that the piezoresistance effect

decreases as doping concentration increases, a trend that is confirmed with experimental measurements.

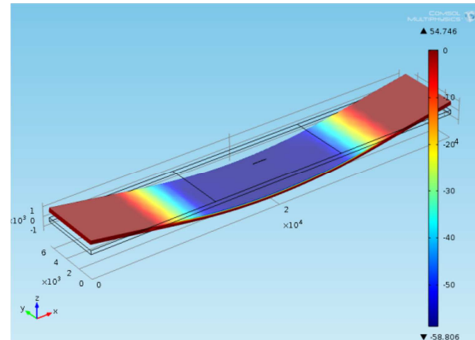


Figure 7: 3D plot of stress tensor in x direction.

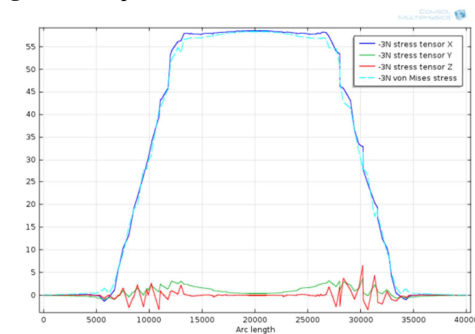


Figure 8: Principal stresses across silicon beam subjected to -3N load.

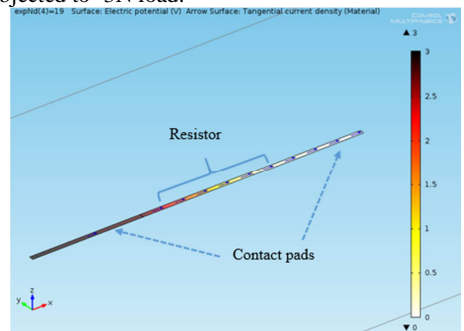


Figure 9: Current density, contours: Electric Potential, supplied with 3V bias.

Figure 11 presents a comparison between COMSOL simulation and experimental work for piezoresistors at four different doping levels i.e. $1.0 \times 10^{19} \text{cm}^{-3}$, $7.6 \times 10^{19} \text{cm}^{-3}$, $1.2 \times 10^{20} \text{cm}^{-3}$ and $1.3 \times 10^{20} \text{cm}^{-3}$. The discrepancies between the simulation and experimental work are generally small. The simulation results over-estimate the piezoresistance effect at $1.0 \times 10^{19} \text{cm}^{-3}$.

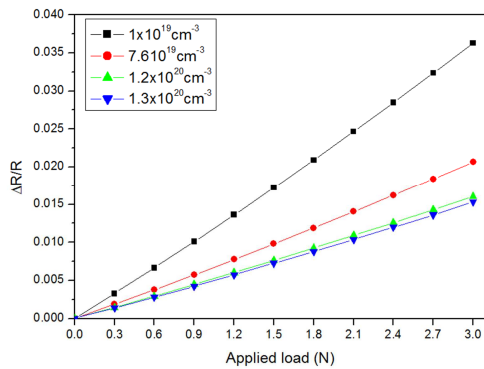


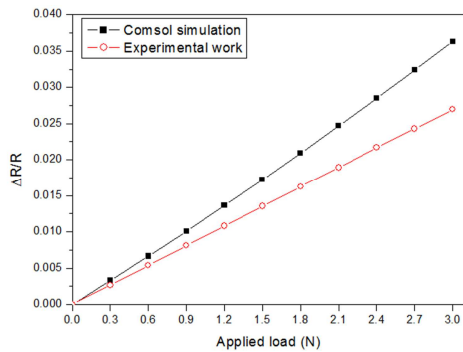
Figure 10: Resistance change vs load applied for a range of doping concentrations.

For heavily doped devices (above $5.0 \times 10^{19} \text{ cm}^{-3}$), COMSOL has under-estimated the piezoresistance effect with less than 20% difference (refer to **Figure 11**). However, for doping concentration at $1.0 \times 10^{19} \text{ cm}^{-3}$, the deviation between simulation and experimental results is higher at around 35%. The discrepancies between the simulated and

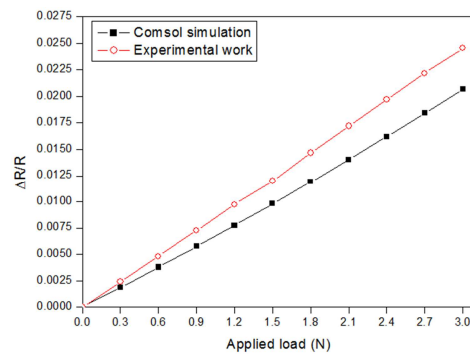
experimental measured results could be due to several factors such as material properties, measurement setup, and force application method. Overall, the simulation results verify that the piezoresistance effect in silicon changes as function of doping.

5. Conclusions

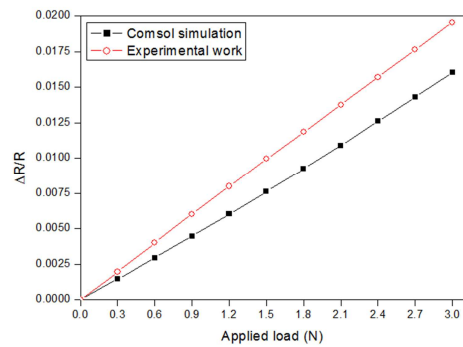
COMSOL Multiphysics was employed to investigate piezoresistive effect in *p*-type silicon for a range of doping concentrations. Simulation results demonstrate a similar trend to experimental results and show that the piezoresistance effect decreases as the doping concentration increases. Four point bending force application method produced uniform and uniaxial stress along the *x* direction. The stress and deflection on the silicon beam using a four point bending setup were also simulated.



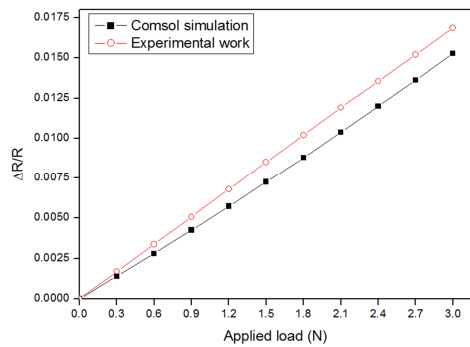
a.



b.



c.



d.

Figure 11: Comparison results between COMSOL simulation and experimental work for piezoresistors doping concentration at a. $1 \times 10^{19} \text{ cm}^{-3}$ b. $7.6 \times 10^{19} \text{ cm}^{-3}$ c. $1.2 \times 10^{20} \text{ cm}^{-3}$ d. $1.3 \times 10^{20} \text{ cm}^{-3}$.

6. References

1. C. S. Smith, "Piezoresistance effect in germanium and silicon," *Physical review* 94, 1, 42(1954).
2. A. A. Barlian, W. T. Park, J. R. Mallon, A. J. Rastegar, & B. L. Pruitt, "Review: Semiconductor piezoresistance for microsystems.", *Proceedings of the IEEE* 97, 3, 513-552 (2009).
3. R. E. Beaty, R. C. Jaeger, J. C. Suhling, R. W. Johnson, & R. D. Butler, "Evaluation of piezoresistive coefficient variation in silicon stress sensors using a four-point bending test fixture," *Components, Hybrids, and Manufacturing Technology, IEEE Transactions on*, 15, 904-914 (1992).
4. E. Lund, & T. G. Finstad, "Design and construction of a four-point bending based set-up for measurement of piezoresistance in semiconductors," *Review of scientific instruments* 75.11, 4960-4966 (2004).
5. J. Richter, M. B. Arnoldus, O. Hansen, & E. V. Thomsen, "Four point bending setup for characterization of semiconductor piezoresistance." *Review of scientific instruments* 79.4 044703-044703 (2008).
6. T. H. Tan, S.J.N Mitchell, D.W. McNeill, P. Baine, J. Montgomery, H. Wadsworth, S. Strahan, & I. Bailie., "Evaluation of the piezoresistance properties of *p*-type silicon," *23rd Micromechanics and Microsystems Europe, Ilmenau, Germany*, (2012).
7. Y. Kanda, "A graphical representation of the piezoresistance coefficients in silicon," *IEEE Transactions on Electron Devices*, pp. 64-70, (1982).
8. S. Beeby, Chapter 5 in "MEMS Mechanical Sensors," Boston: Artech House Academic Press, (2004).

7. Acknowledgements

T.H. Tan wishes to thanks Schrader Electronics Ltd. for financial support for the project.